Molecular Therapy
Original Article

Safety and Long-Term Efficacy of AAV4 Gene Therapy in Patients with *RPE65* Leber Congenital Amaurosis

Guylène Le Meur,[1,2] Pierre Lebranchu,[1,5] Fanny Billaud,[1] Oumeya Adjali,[2] Sébastien Schmitt,[3] Stéphane Bézieau,[3] Yann Péréon,[4] Romain Valabregue,[6] Catherine Ivan,[1] Christophe Darmon,[2] Philippe Moullier,[2] Fabienne Rolling,[2] and Michel Weber[1,2]

[1]Ophthalmology Department, University Hospital Centre (CHU) de Nantes, Nantes, France; [2]INSERM UMR 1089, University of Nantes, CHU de Nantes, Nantes France; [3]Department of Genetics, CHU de Nantes, Nantes, France; [4]Reference Centre for Neuromuscular Disorders, FILNEMUS, CHU de Nantes, Nantes, France; [5]UMR 6597 CNRS, Image and Video Communication Team, Institute for Research into Communications and Cybernetics of Nantes, Polytech Nantes, Nantes, France; [6]Institut du Cerveau et de la Moelle épinière ICM, Centre for NeuroImaging Research (CENIR), Paris, France

The aim of this study was the evaluation of the safety and efficacy of unilateral subretinal injection of the adeno-associated vector (AAV) serotypes 2 and 4 (AAV2/4) RPE65-*RPE65* vector in patients with Leber congenital amaurosis (LCA) associated with *RPE65* gene deficiency. We evaluated ocular and general tolerance and visual function up to 1 year after vector administration in the most severely affected eye in nine patients with retinal degeneration associated with mutations in the *RPE65* gene. Patients received either low (1.22×10^{10} to 2×10^{10} vector genomes [vg]) or high (between 3.27×10^{10} and 4.8×10^{10} vg) vector doses. An ancillary study, in which six of the original nine patients participated, extended the follow-up period to 2–3.5 years. All patients showed good ophthalmological and general tolerance to the rAAV2/4-RPE65-*RPE65* vector. We observed a trend toward improved visual acuity in patients with nystagmus, stabilization and improvement of the visual field, and cortical activation along visual pathways during fMRI analysis. OCT analysis after vector administration revealed no retinal thinning, except in cases of macular detachment. Our findings show that the rAAV2/4.RPE65.RPE65 vector was well tolerated in nine patients with *RPE65*-associated LCA. Efficacy parameters varied between patients during follow-up.

INTRODUCTION

Leber congenital amaurosis (LCA) is a severe and early form of retinal degeneration that accounts for 5% of retinal dystrophy cases. LCA was first described in 1869 by the German ophthalmologist Theodor Leber,[1] who described severe visual impairment beginning at or within 1 month of birth, characterized by nystagmus, amaurotic pupils, and retinitis pigmentosa. A non-detectable or highly attenuated electroretinogram (ERG) is a key diagnostic feature.[2] Visual difficulties are generally identified by 6 months of age. LCA is a heterogeneous genetic disease; 21 affected genes, expressed mainly in photoreceptors or the retinal pigmented epithelium (RPE), have been identified to date.[3] The *RPE65* gene, responsible for 6% of LCA cases,[4] encodes a 65-kDa isomerase that participates in the visual cycle.[5] RPE65 protein deficit induces early degeneration of photoreceptors cells.[6] No treatment for this retinal pathology is currently available. In recent years, several clinical trials have examined the potential of gene therapy strategies for the treatment of LCA associated with *RPE65* mutations. These studies have shown that subretinal injection of a serotype 2/2 adeno-associated vector (AAV) carrying the *RPE65* gene results in improved retinal sensitivity, visual acuity, pupillomotor reflex, nystagmus, microperimetry parameters, and mobility test performance, especially in low lighting conditions, over follow-up periods of 2–3 years.[7–11] However, continued retinal degeneration has been reported in other gene therapy studies with follow-up periods exceeding 3 years.[12,13] Bilateral injection of an AAV2/2-*RPE65* vector appears to be a safe procedure that induces a mild, non-toxic immune reaction.[14] All trials performed to date have evaluated the effects of serotype 2 AAV vectors, which target pigmented epithelium cells and retinal cells. By contrast, serotype 4 AAV vectors have a specific tropism for RPE cells.[15]

Here, we report the results of a phase 1/2 study performed at Nantes University Hospital that evaluated the efficacy of and tolerance to a type 2/4 AAV vector carrying the *RPE65* gene under the control of the RPE65 promoter.

RESULTS

Demographic and Surgical Data

Participating patients were aged 9–42 years (Table 1) and all carried *RPE65* gene mutations (Table S1). The follow-up period was 1 year. Of the nine patients who underwent follow-up, six volunteered for additional follow-up for periods ranging from 2 to 3.5 years

Received 16 March 2017; accepted 9 September 2017;
https://doi.org/10.1016/j.ymthe.2017.09.014.

Correspondence: Guylène Le Meur, PhD, MD, Ophthalmology Department, CHU de Nantes, CHU Hôtel Dieu, 1 place Alexis Ricordeau, 44093 Nantes Cedex 01, France.
E-mail: guylene.lemeur@univ-nantes.fr

Table 1. Surgical and Injection Data

		Age (Years)	Volume	Vector Genomes	Injection Number	Follow-up
First cohort	CG01	28	330 μL	2.01×10^{10}	2	1 year
	BJ03	27	200 μL	1.22×10^{10}	3	1 year
	MM04[a]	35	300 μL	1.83×10^{10}	3	3 years 5 months
Second cohort	MR05[a]	42	700 μL	4.27×10^{10}	5	2 years
	HM06[a]	22	770 μL	4.7×10^{10}	2	3 years
	HT07[a]	20	530 μL	3.23×10^{10}	4	3 years 2 months
Third cohort	AM08[a]	19	700 μL	4.27×10^{10}	4	2 years 6 months
	HM09	15	800 μL	4.8×10^{10}	4	1 year
	LC10[a]	9	770 μL	4.7×10^{10}	3	2 years 2 months

[a]Patients who underwent long-term follow-up.

post-injection (Table 1). The severity of retinal detachment varied from one patient to the next. Injection volume also varied between patients (200–800 μL), with doses ranging from 1.22×10^{10} to 4.8×10^{10} vector genomes (vg) (Table 1). Subretinal injections were administered simultaneously in two to five injection sites (Table 1). Injection sites were selected to primarily target the extra-foveal and peripheral retinal regions. In patients MM04, HM06, and HT07, subretinal blebs merged together during administration. For patient MM04, the macula and the fovea were detached by the subretinal injection. For patients HM06 and HM09, the border of the bleb was close to the fovea without detaching it. Subretinal fluid was absorbed between 24 hr and 4 days post-injection.

Systemic Tolerance to AAV2/4-RPE65-*RPE65*

During the course of the trial, no adverse events associated with the AAV2/4-RPE65-*RPE65* vector were recorded in the "safety@easy" vigilance database. Two serious adverse events that were unrelated to the test product were declared: one thyroidectomy and one supraventricular tachycardia. No clinically relevant changes in hematological or biochemical parameters were detected during follow-up.

During the biodistribution study, the viral vector was primarily detected in post-operative nasal samples, peaking at D+2. The majority of viral vector values were below the limit of quantification (LOQ) of the assay. Only patient LC10 showed values that exceeded the LOQ threshold at D+2 and D+3, with a maximum value of 201 copies detected in lachrymal secretions at D+2. As regards viral dissemination in the blood, viral vector was transiently detected only in patient HM09 between D0 and D+3, with all values remaining below the LOQ (38, 40, and 32 copies detected in 14 μL of serum analyzed at D+1, D+2, and D+3, respectively) (Table S2). No urinary dissemination was detected in any of the nine patients during monitoring. All patients left the containment chamber by D+3.

Six patients did not show detectable AAV4 immunoglobulin G (IgG) antibodies in the serum either before injection or after injection of the recombinant AAV (rAAV)2/4-hRPE65 product. We detected anti-AAV4 IgG antibodies in three patients. One patient (MR05) revealed stable anti-AAV4 IgG antibodies titers before and after injection, without significant increase after injection. Two patients (MM04 and HM09) appeared negative before AAV4 injection with detectable anti-AAV4 IgG antibodies in the serum only following vector subretinal administration (as soon as D14 after injection) (Table S3). Regarding the detection of neutralizing factors, the results were correlated to anti-vector IgG antibodies. Indeed, one patient (MR05) revealed stable titers (1/50) of detectable anti-AAV4 neutralizing factors (NFs) before and after injection, without any increase after subretinal vector administration. Two patients (MM04 and HM09) were negative before AAV injection and showed detectable NFs after injection similarly to IgG antibodies, with the highest titers observed at days 30 and 120 for HM09 and MM04 patients, respectively. In contrast to the humoral response, anti-AAV4 cellular immunity was observed only in one patient (MM04). Indeed, a statistically significant positive interferon-γ (IFN-γ) response was observed against both peptide pools 1 and 2 at all time points with no significant increase in the intensity of the response (Table S3). Regarding RPE65 cellular immunity, all the patients were found to be negative except MM04, who showed a weak and transient cellular response to RPE65 between days 14 and 60 following vector delivery.

Local Tolerance to AAV2/4-RPE65-*RPE65*

Ophthalmological follow-up of the nine injected patients revealed no deleterious effects (i.e., no chronic inflammation, no retinal detachment, no chorioretinal abnormality, and no cataracts). In the tolerance questionnaire, most patients reported a painful tingling sensation in the treated eye during the immediate post-operative period. This discomfort persisted for only a few days.

No inflammation was evident in the biomicroscopic examination. Nonetheless, laser flare meter (LFM) analysis revealed infra-clinical inflammation at D+4 in three patients (HT07, HM09, and LC10), with levels returning to normal by D+14 (Figure 1A). With a flare value of 35.9 ± 7.4 photons (Ph)/ms at D+4, patient HT07 required an increase in local anti-inflammatory treatment (six times per day), which resulted in rapid normalization of LFM values. More significant inflammation was observed in patients HM09 and LC10: flare

A

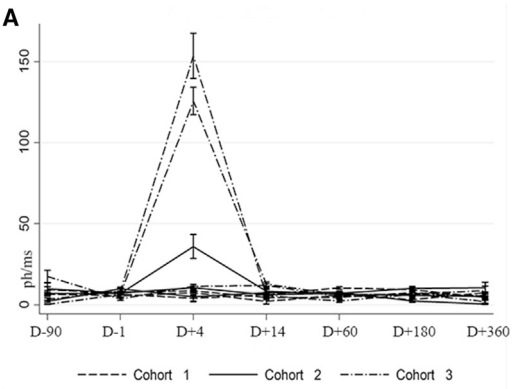

B

	D+4	D+14
HT07	35.9 +/- 7.4	7.8 +/- 1.8
HM09	125.7 +/- 8.5	12.7 +/- 1.3
LC10	153.6 +/- 13,9	5.7 +/- 1.3

Figure 1. Evaluation of Post-injection Inflammation

(A) Laser flare meter analysis of treated eyes (Ph/ms) at D−90, D−1, D+4, D+14, D+60, D+180, and D+360. (B) Laser flare meter values (Ph/ms) for the three patients exhibiting inflammation.

values of 125.7 and 53.6 Ph/ms, respectively, were recorded at D+4, but returned to normal values by D+14 without need for increased local anti-inflammatory treatment (Figure 1B). These two patients received high doses of vector (800 and 770 μL, respectively). In patient LC10, retinal detachment in the bleb area took longer to resolve (4 days) than in the other patients (24 hr).

Chorioretinal imaging (retinophotography, autofluorescence, fluorescein angiography, or indocyanine green angiography) revealed no choroidal or vascular retinal abnormalities in or around the injected retinal areas. The only alteration observed was the development of an atrophic scar on the RPE at the retinotomy site, characterized by a "window effect" in the fluorescein angiography.

Spectral domain optical coherence tomography (SD-OCT) analysis of mean retinal thickness 1 or 2–3 years post-injection revealed no alterations in retinal thickness in treated or untreated eyes (Figure 2A). In patient MM04, the total retinal thickness of the treated eye decreased between the two time points (before injection and 1 year post-injection) (Figure 2B). However, assessments performed 3 years post-injection revealed no further reduction in total retinal thickness, with values remaining stable between 1 and 3 years post-injection. In patient MM04, no alterations in the retinal thickness of the untreated eye were observed over the three time points analyzed (Figure 2B). In the two patients with the bleb close to the fovea, no alteration in total retinal thickness in the central 600-μm area was observed over the course of follow-up (Figures 2C and 2D).

Efficacy of AAV2/4-RPE65-*RPE65*

Responding to a questionnaire, four of nine patients reported improved perception of detail, three of nine reported improved fixation, one of nine reported improved color vision, one of nine reported reduced photophobia, and one of nine reported reduced visual fatigue. Six out of nine patients presented nystagmus (Figure 3A) and four presented divergent strabismus (Figure 3A) upon inclusion in the study. Patient HM06 presented with exotropia, with the untreated eye dominant. Following subretinal vector injection, dominance switched to the treated eye. Patient HT07 reported that he preferred using only the treated eye for close-range vision, whereas patient MR05 reported a sensation of ocular dominance in the treated eye.

The clinical progression of visual acuity loss varied between patient cohorts (Figure 3A). In cohort 1 (baseline visual acuity <10 Early Treatment Diabetic Retinopathy Study [ETDRS] letters), no alteration in visual acuity was observed; in cohort 2 (baseline visual acuity between 7 and 31 ETDRS letters), a trend toward improved visual acuity was observed; and in cohort 3 (baseline visual acuity >50 ETDRS letters with no nystagmus), no alteration was observed (Figure 3A). We observed a non-significant improvement in average visual acuity 1 year post-injection (+2.5 letters for all treated eyes, except in patient CG01, whose initial VA was not quantifiable; $p = 0.49$). Even though the improvement was not statistically significant, it was greater in the case of eyes with nystagmus (+7.6 letters on average for the first five patients with nystagmus; $p = 0.125$): a slit-lamp examination and live infrared OCT imaging revealed a post-treatment reduction in the amplitude of nystagmus in these patients. General analysis of visual acuity of patients during follow-up revealed that mean visual acuity remained stable in the treated eye (+2.5 letters at 1 year and +2.3 letters at 2–3 years), whereas a trend toward reduced visual acuity was observed in untreated eyes (+1 letter at 1 year [$p = 0.79$] and −4.2 letters at 2–3 years [$p = 0.20$]) (Figure 3B). None of the alterations in visual acuity were statistically significant (Figure 3C).

Alterations in the surface area of the visual field varied between patients: measurement of the surface area of the V4 visual area revealed an increase for five patients (CG01, BJ03, HM06, HT07, and AM08), a decrease for two patients (MM04 and HM09), and no change for two patients (MR05 and LC10) (Figures 4A and 4B). At 3 years of follow-up, four of the six patients evaluated showed an increase in the surface area of the visual field as compared with pretreatment values (multiplication ratio range, 0.7–5.9) (Figure 4B). A slight reduction in the surface area of the V4 isopter of the untreated eye was observed over long-term follow-up (Figure 4B). No significant alterations in "loss variance" (LV) or "mean deviation" (MD) of the automated visual field were observed at either 1 year or >2 years of follow-up.

Microperimetry analysis at 1 year post-injection revealed that the average sensitivity and number of microscotomas in both treated and untreated eyes remained stable (Figures 5A and 5B). Similar findings were obtained for microperimetry analysis performed at 2–3 years (Figures 5C and 5D). No improvements in ERG or pupillometry results were observed after subretinal injection of the AAV2/4.RPE65 vector. No modification in retinal autofluorescence was detected. In the mobility test, comparison of pre-injection and 1 year

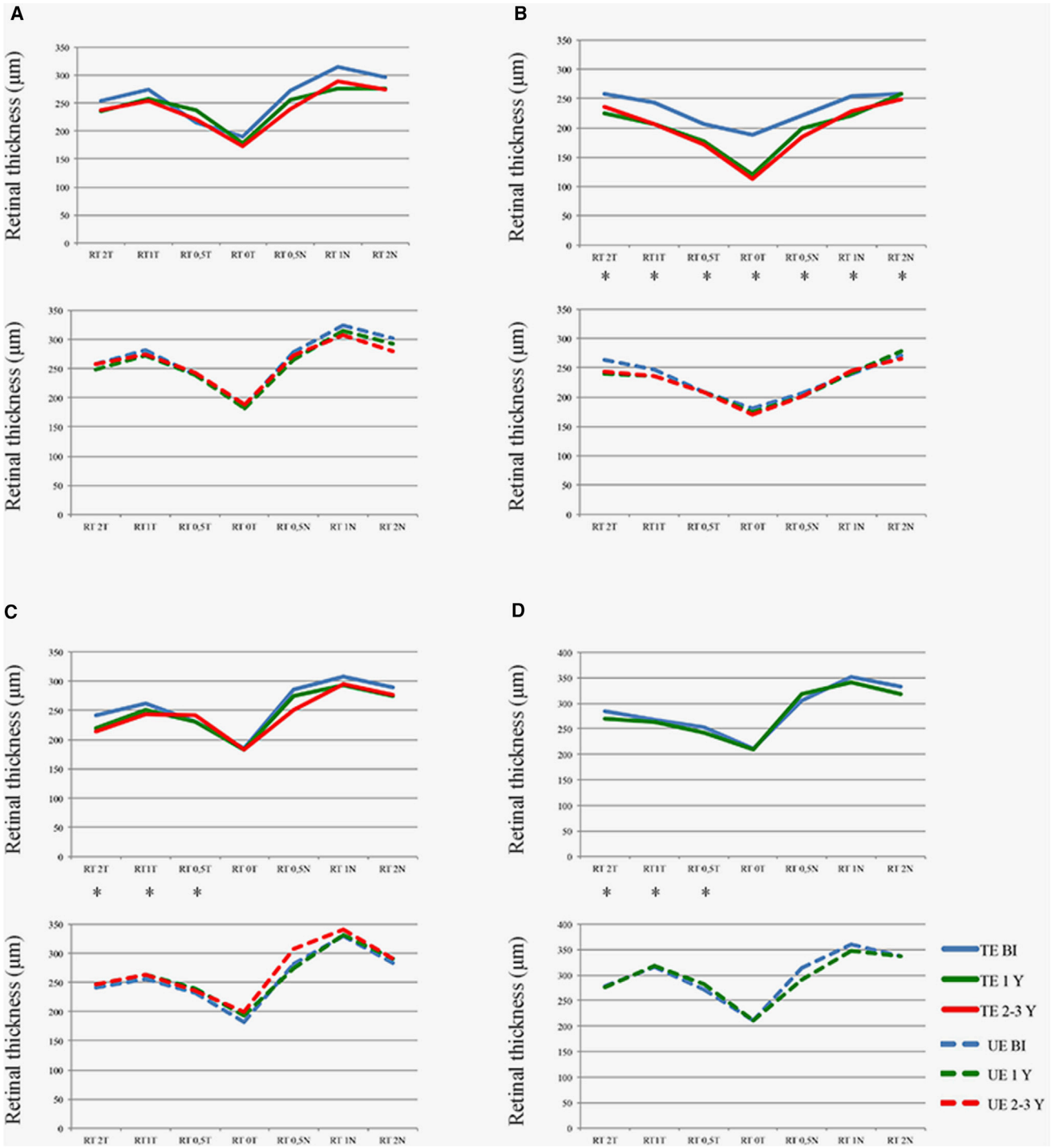

Figure 2. SD-OCT Evaluation of Changes in Total Retinal Thickness according to Eccentricity of the Fovea

SD-OCT evaluation of changes in total retinal thickness according to eccentricity of the fovea was measured in treated eyes (upper graphs, solid line) and untreated eyes (lower graphs, dotted line) at baseline (blue line), 1 year post-treatment (green line), and 2–3 years post-treatment (red line). (A) Mean retinal thickness in all patients. (B) Patient who experienced foveal detachment during surgery (MM04). (C) Patient with the bleb close to the fovea (HM06). (D) Patient with the bleb close to the fovea (HM09). BI, before injection; N, nasal; T, temporal; TE, treated eye; UE, untreated eye; Y, year, Asterisks (*) indicate subretinal injection site.

A

	Treated Eye			Untreated Eye			Nystagmus	exotropia
	BI	1 year	2-3 years	BI	1 year	2-3 years		
CG01	LP	LP	NA	LP	LP	NA	+	+
BJ03	6	10	NA	10	23	NA	+	+
MM04	8	7	0	31	33	24	+	+
MR05	31	39	33	43	40	41	+	-
HM06	31	46	43	37	29	39	+	+
HT07	7	19	17	20	24	3	+	-
AM08	56	42	57	66	64	67	-	-
HM09	54	50	NA	57	59	NA	-	-
LC10	59	59	56	65	65	63	-	-

B

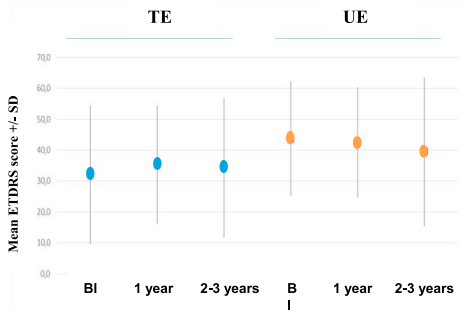

C

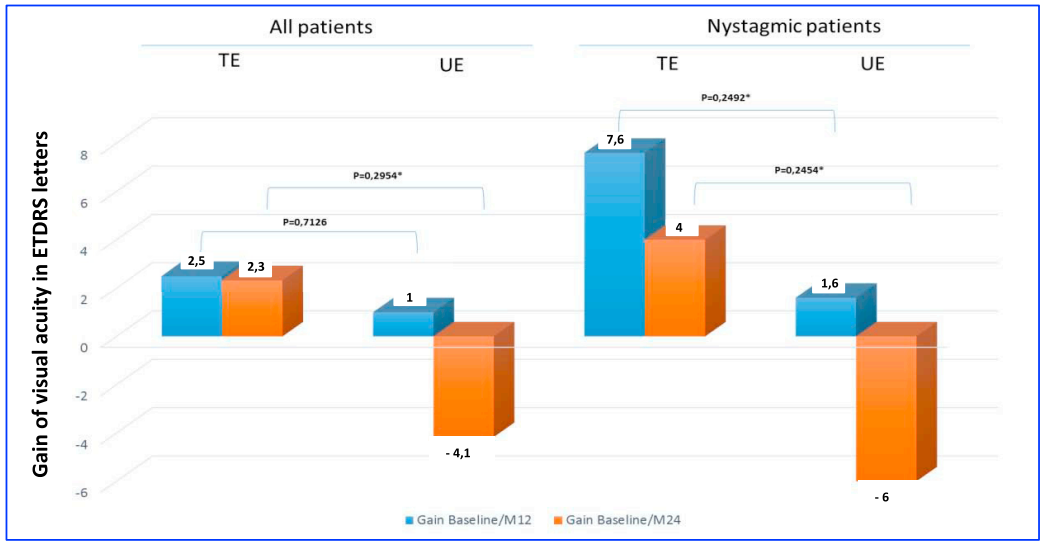

Figure 3. Visual Acuity Measured in Treated Eyes and Untreated Eyes at 1 (Blue) and 2–3 Years (Orange) Post-injection

(A) ETDRS visual acuity of injected and uninjected eyes before injection, 1 year post-injection, and at the final examination. (B) Mean visual acuity in the six patients who underwent long-term follow-up. (C) Changes in mean visual acuity after the surgery as measured in the untreated and treated eyes in the six patients who underwent long-term follow-up. Data are shown for all patients (left) and for nystagmic patients only (right). BI, before injection; LP, light perception; TE, treated eye; UE, untreated eye.

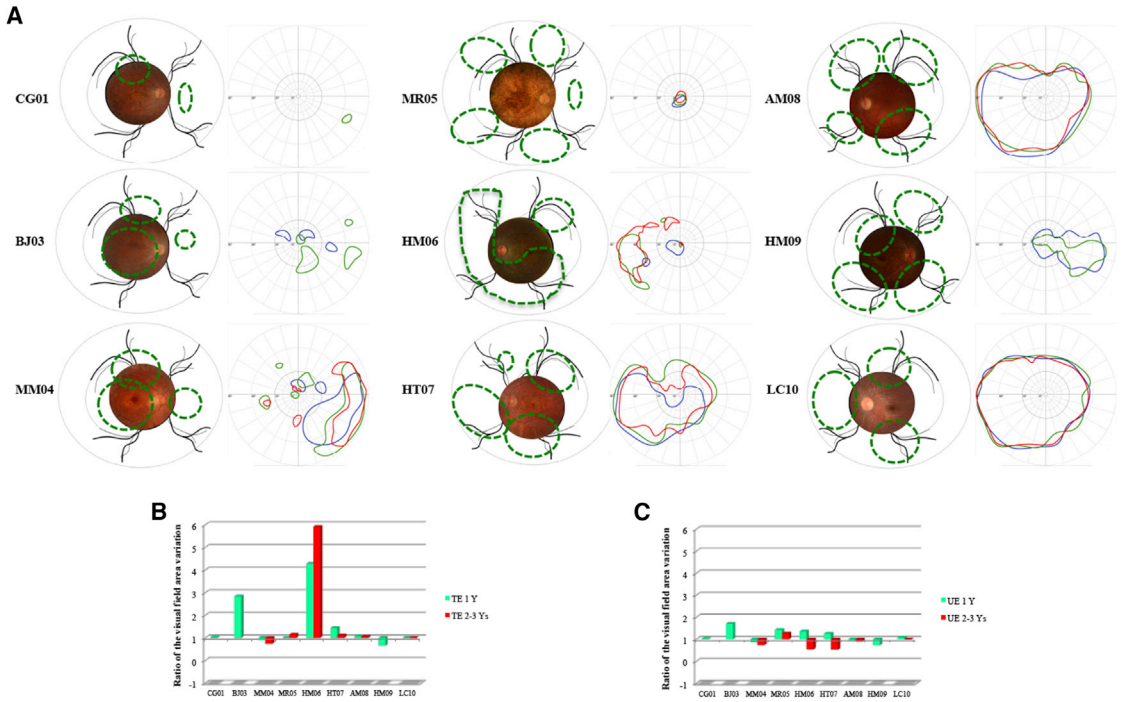

Figure 4. Visual Field Analysis during Follow-up

(A) For each patient a composite retinal photograph is shown (left): the area exposed to the vector is indicated with a green line. The Goldmann visual field is shown on the right: blue lines delineate the V4 surface before injection, green lines indicate the V4 surface 1 year post-injection, and red lines indicate the V4 surface at the final follow-up examination. (B) Variation in the visual field surface area of the treated eye: 1 year post-treatment versus values obtained at final follow-up examination. (C) Variation in the visual field surface area in untreated eye: 1 year post-treatment versus values obtained at final follow-up examination. TE, treated eye; UT, untreated eye; Y, year.

post-injection values revealed no significant differences in transit time or percussions between the treated and untreated eyes.

fMRI Results following Sub-retinal Injection of the AAV2/4-RPE65-*RPE65* Vector

Cortical activity in the primary visual cortex increased following light stimulation as compared with basal conditions (resting in darkness) (Figure 6A). The average T signal increased with luminance (one-way ANOVA: $F_{5,186} = 5.97$; $p < 0.0001$). The average T signal also differed between patients (one-way ANOVA: $F_{7,176} = 13.23$; $p < 0.00001$) (Figure 6B).

A multivariate ANOVA with three factors (patient, treated versus control eye, pre- versus post-treatment) revealed significant differences in activation among patients ($p < 0.0001$) and a significant subject × laterality interaction ($p < 0.0001$). For both the control and treated groups, no significant difference in pretreatment versus post-treatment levels of activation was observed. Finally, the three-way interaction that searches more specifically for a significant modification of activation in a subject according to treatment did not reveal a statistically significant difference either.

Random effect group analysis, which enables identification of activations significantly present after treatment, identified no cluster for the lowest lighting conditions (C1 and C2). For higher luminance values, we detected one to four clusters depending on the stimulation conditions of the treated eye, as compared with only one or two clusters for the untreated eye (Table S4). In the group analysis, all confounded stimulation conditions confirmed the onset of activation after treatment of the treated eye, whereas no activation was detected for the control group. We therefore identified three clusters in which activity was significantly greater after than before treatment. All clusters were located within the white matter. The most significant cluster was located just behind the ipsilateral lateral geniculate ganglion: its lateral-most voxel was 70% likely to belong to the optic radiation, whereas its most medial voxel was 66% likely to belong to the posterior corpus callosum (Juelich Histological Atlas). The most significantly activated voxel of the second cluster was 89% likely to belong to the corpus callosum. The final cluster was located within the anterior lobe of the cerebellum (Figure 6C).

DISCUSSION

This gene therapy trial assessed the safety and efficacy of the AAV2/4-RPE65-*RPE65* vector, which is specific for the retinal epithelium, in patients with LCA associated with *RPE65* deficiency. We observed no local or systemic adverse effects, in line with the findings of several previous clinical trials of the AVV2/2 vector.[7,9–11,16]

The formation of several subretinal blebs as a consequence of two to five retinotomies was not associated with any adverse effects.

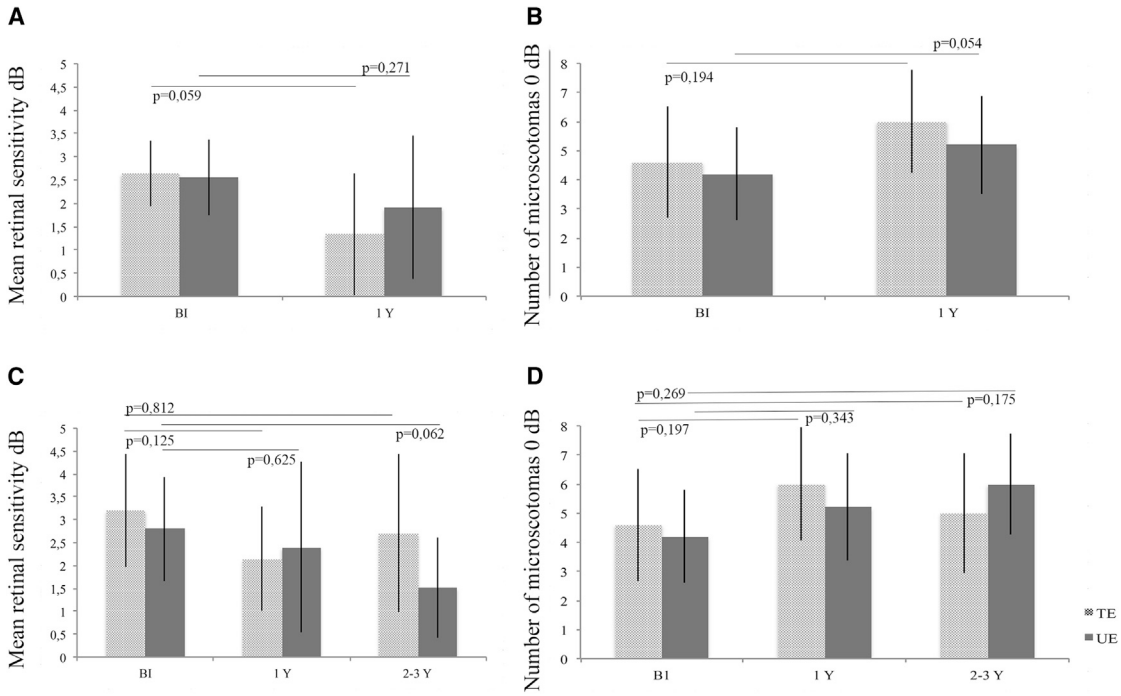

Figure 5. Microperimetry Data for All Patients at 1 Year Post-injection and for Patients Who Underwent Long-Term Follow-up

(A) Mean retinal sensitivity at 1 year post-injection. (B) Number of microscotomas at 1 year post-injection. (C) Mean retinal sensitivity in patients who underwent long-term follow up. (D) Number of microscotomas in patients who underwent long-term follow-up. Treated and untreated eyes are represented by light gray and dark gray bars, respectively. BI, before injection; Y, year.

Evaluation of post-operative ocular inflammation revealed no clinical abnormalities, although LFM showed a mild, transient increase in protein flare (flare < 150 Ph/ms at D+4) in three of six patients injected with the highest dose with a normalization at D+14. In line with these findings, previous gene therapy trials of LCA patients reported mild, transitory intra-ocular inflammation in three patients who received a dose of 1×10^{12} vg,[12] and grade 0.5 inflammation in two patients between 7 and 14 days post-treatment.[11] Even if this inflammation is related to gene therapy, it is minimal and inconsequential, and is also observed after vitrectomy for rhegmatogenous retinal detachment,[17] peaking 1 week after surgery, and even more so in patients with retinitis pigmentosa.[18]

Biodistribution of the viral vector was assessed following subretinal injection. Vector was detected in nasal secretion samples: values exceeded the LOQ only in one patient (LC10), peaking at D+2. In serum samples, the vector was only detected in a single patient at D+2, at levels below the LOQ. In previous preclinical studies performed in large animals, we observed similar biodistribution kinetics in nasal and tear samples.[15] However, we also detected the vector in serum samples up to 25 days post-injection,[15] a finding that was not replicated in the present study. Detection of vector DNA in human tear and blood samples a few days post-injection has only been reported in the Bennett et al.[14] and Maguire et al.[16] studies.

Our immunological findings suggest that the positive humoral response observed in patient MR05 was unrelated to injection of the viral vector per se and more likely due to pre-existing anti-AAV4 immunity. Nonetheless, we cannot rule out potential cross-reactivity caused by previous immunization against another AAV serotype. Further supporting this possibility, MR05 was the oldest patient in the cohort (43 years at the time of injection). By contrast, the results of our analyses of anti-AAV4 IgG and NF levels in patients MM04 and HM09 suggest that the observed kinetics are related to rAAV2/4-hRPE65 injection. The lack of correlation between humoral and cellular data in our patient cohort is in line with previous studies using AAV1[19] and AAV2.[20] This may be because of differences in the sensitivity of humoral and cellular assays, and/or the higher level of cross-reactive responses for T cells versus antibodies. The anti-AAV4 response observed in our study was consistent with the findings of other retinal AAV-based clinical trials in which both humoral and cellular responses were reported in certain patients.[9,14,21–23] These responses were generally mild and/or transient, and they did not preclude injection of the contralateral eye.[14] Regarding RPE65 humoral immunity, we were unfortunately unable to draw any conclusions. It is important to note that in other AAV2-based clinical trials of LCA, detection of anti-RPE65 IgG by ELISA was either not reported[23] or the results were similar to ours, with high levels of reactivity.[14,22] Bennett and coworkers[14] detected anti-RPE65 antibodies in two patients, both in baseline samples and after vector administration. They hypothesized that these positive results may have been

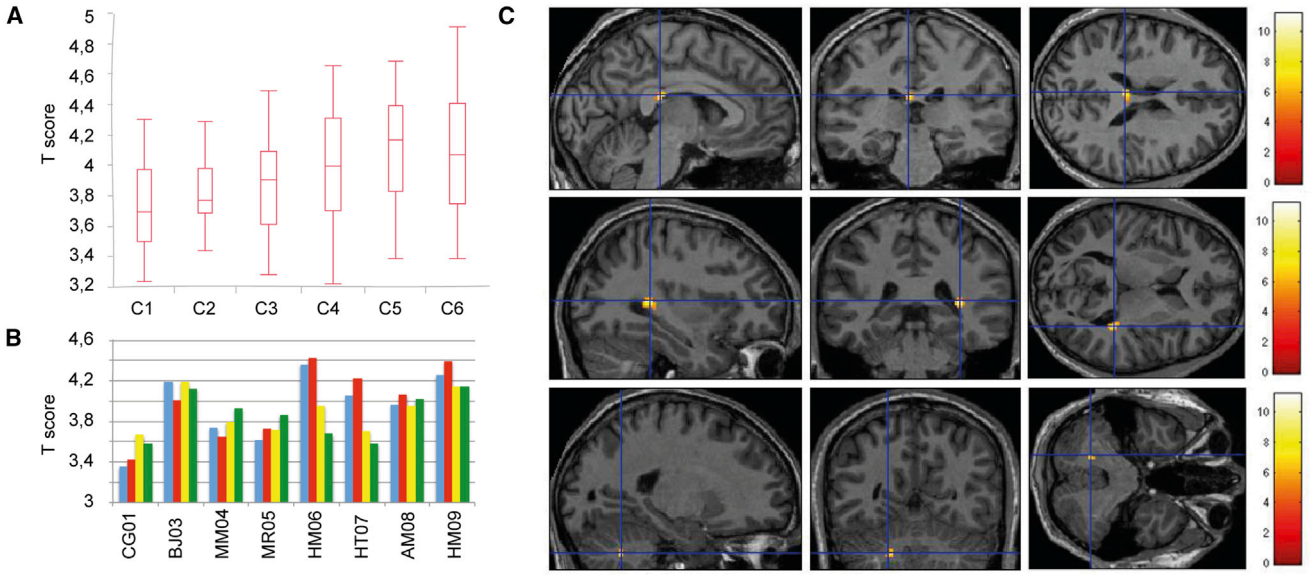

Figure 6. Functional MRI Analysis

(A) Activity in the primary visual cortex as a function of the intensity of light intensity of stimulation. T score is based on the stimulation conditions (C1, lowest luminance; C6, highest luminance), as illustrated in the boxplot. (B) Primary visual cortex activity in individual patients. The mean T score per patient is shown. Blue, treated eye before treatment; red, treated eye after treatment; yellow, untreated eye before treatment; green, untreated eye after treatment. (C) Increase in activity after treatment. Statistical parametric map showing the voxels with a significant activation ($p < 0.001$ uncorrected, cluster correction at $p < 0.05$, random effect; $n = 8$) after versus before treatment, all stimulation conditions together, projected onto a mean MRI template. Color bar indicates t scores.

caused by cross-reaction with another RPE65-like protein or production by the patients in question of a dysfunctional but immunologically detectable protein. Taken together, our ELISpot results were consistent and suggest a low and transient cellular response against RPE65 in patient MM04 between 14 and 60 days after vector delivery. In agreement with our findings, a transient response was also reported in another AAV-based LCA trial, in which two patients tested positive for anti-vector antibodies 30 days after subretinal AAV2 administration.[22] In a more recent study, two patients who had previously received a single, unilateral AAV2 vector injection tested positive between 4 and 6 weeks after injection of the contralateral eye with the same AAV2 vector.[14]

In terms of treatment efficacy, the results of functional tests revealed variable modifications after treatment. While improvements in visual acuity were not significant for all patients, we nonetheless observed more marked improvements in visual acuity in patients from cohort 2, who presented nystagmus and intermediate initial visual acuity upon inclusion in the study. By contrast, patients from cohort 3 (without nystagmus and with correct initial visual acuity) showed less marked improvements in visual acuity. The better outcomes observed in cohort 2 may be related to the clinical modification in nystagmus. Improvements in visual acuity have been reported in other *RPE65* gene therapy trials,[7,11,16] in some cases persisting up to 3 years post-treatment.[8] Testa and coworkers[8,21] reported a correlation between a reduction in nystagmus and increased visual acuity,[8] with a reduction in the amplitude of the nystagmus.[21] In their study of infantile nystagmus syndrome, Dell'Osso and coworkers[24] reported a correlation between visual acuity and foveation quality. Similarly, an increase in foveation time has been proposed to improve visual acuity in nystagmus patients.[25] In future studies it will be important to measure both fixation and the kinetic characteristics of nystagmus in order to quantify modifications in nystagmus in patients treated with gene therapy.

The effects of rAAV2/4.RPE65.*RPE65* treatment on the visual field varied between patients. Over 2 years of follow-up, the surface area of the visual field increased in six patients, decreased in two patients, and remained stable in one patient. The therapeutic effect of rAAV2/4.RPE65.*RPE65* likely depends in part on the amount of RPE65 protein produced, and therefore on the dose of injected viral vector in vg/mL (which influences the percentage of RPE cells transduced), as well as the surface area of detached retina (which in turn influences the surface area of RPE transduced). In our study, patients received several simultaneous subretinal injections in order to treat the largest possible retinal surface area, in accordance with the injection volumes stipulated in the protocol. Patients in cohorts 2 and 3 (total volume < 800 μL) received more injections (4–5 blebs) than those in cohort 1, increasing the contact between the viral vector and the retinal surface. The number of injection sites in our trial was higher than that reported in the studies conducted by Maguire et al.[16] or Weleber et al.[11] (single injection of 450 μL), Jacobson et al.[13] (maximum dose of 450 μL in two injections), or Bainbridge et al.[12] (single injection of 1 mL). It therefore remains unclear whether our approach provides any significant benefit. Treatment efficacy is also associated with vector concentration, the state of degradation of the retina, the type of

mutation (missense or stop codon mutation), and the patient's age. In cohort 3, in which initial visual function was better preserved, no alterations in visual function were observed for either the treated or untreated eyes. We were unable to determine the impact of age on the visual field improvement in our series of nine patients, only two of whom were pediatric subjects. By contrast, Bainbridge et al.[12] observed more significant visual field improvements in patients aged approximately 20 years, whereas Maguire and coworkers[16] reported visual field improvements in the youngest patients. Compared with previous studies, the doses increment in our trial was smaller. Moreover, the doses of vg injected ($1{,}22 \times 10^{10}$ to 4.8×10^{10}) were lower than those injected in other studies (ranging from 1.5×10^{10} vg[16] to 6.11×10^{11} vg[11]). Our highest dose administered was only double the lowest dose, and therefore the dose per cell was unchanged. As suggested by the findings of Koch et al.,[26] this dose may have been insufficient to generate sufficient protein to produce a functional visual benefit or to prevent further retinal degeneration.

The aforementioned functional modifications were observed within several months of vector delivery. However, further analysis of these functional alterations over a longer duration will be necessary to demonstrate a persistent gene therapy effect, particularly in light of recent findings describing a diminished benefit of *RPE65* gene therapy after 3 years of follow-up.[12]

Our SD-OCT analysis of total retinal thickness revealed minimal reduction in foveal and perifoveal thickness in eyes in which the bleb extended in the subfoveal area. This effect was observed within the first few months following treatment and remained stable over time. Similar observations have been reported in other trials of gene therapy for the treatment of *RPE65*-related LCA or choroideremia.[27] The reduced thickness does not worsen throughout follow-up at 1 or more than 2 years. It could be the consequence of macular detachment as observed in detachments of macula-off retina, which have a worse visual prognosis than macula-on retina,[28,29] which appears correlated to whether or not there is an intact EZ line post-operatively.[30] However, we observed no alterations in total macular retinal thickness at either 1 or 2+ years post-injection, in contrast to the findings of both Bainbridge et al.[12] and Jacobson et al.,[13] who attributed the progressive decrease in retinal thickness to the pursuit of retinal degeneration. We cannot rule out the possibility that further retinal thinning may occur in our patients, and we plan to assess this with continued follow-up.

In contrast to our findings in *RPE65*$^{-/-}$ Briard dogs treated with the same vector serotype (AAV 2/4),[31] ERG revealed no modification in retinal electrical activity in treated patients. These findings are in agreement with those reported in other gene therapy trials.[7,10,12,14]

Patients with a visual handicap in relation to a *RPE65*$^{-/-}$ mutation present cortical responses to visual stimulation even in the case of significant deficit (first three patients). These responses recorded at the primary visual cortex are correlated to the intensity of visual stimulation, in accordance with the study by Aguirre et al.[32] The absence of modification in cortical activity after treatment reinforces the absence of immediate harmful effect on visual perception. However, infantile abnormal visual perception results in definitive visual cortex disorganization if not treated before the end of the critical period.[33] If retinotopic organization of the visual cortex seems to be preserved even in the case of profound congenital blindness,[34] it results in in-depth anatomic and functional modifications: shrinking of the striated and extra-striated visual cortex surface, increased cortical thickness of the striated cortex, modification of anatomic and functional connections, etc.[35] These modifications are probably not reversible at adult age,[33] which could explain the absence of increased visual cortical activity after treatment.

However, this treatment is associated with increased activity at the white matter in areas involved in the transfer of visual information: ipsilateral optical radiation and posterior corpus callosum. Patients with retinal dystrophy present disorganization of optical radiation while the thickness of ganglion cells (retinal nerve fiber layer [RNFL]) is normal.[36] The origin of this disorganization is probably due to the abnormal visual stimulation, leading to abnormal myelination.[37] The anatomy of the corpus callosum is also modified in case of congenital blindness with atrophy of the posterior part (splenium).[35] Activations of the white matter on fMRI can be observed at this splenium during visual tasks,[38] translating the transfer of inter-hemispheric information between visual cortices. Finally, it was recently revealed that gene therapy treatment could enable improving the organization of ipsilateral optical radiation and posterior corpus callosum.[39] Our study revealed that 6 months after gene therapy there is increased operation of the visual pathways, especially in two areas (optical radiations and splenium) that appear to reorganize after treatment.[39] Improved detection of the retinal signal after gene therapy could increase stimulation of visual pathways leading to reorganization of connections or increased myelinization.[37] These anatomic modifications would account for the increased functional activity identified in this study.

Conclusions

In summary, the data obtained in this clinical trial of AAV2/4.RPE65.*RPE65* treatment of patients with LCA associated with a *RPE65* gene mutation indicate that it can be safely used for both general and ophthalmological purposes. Improvements in visual function varied between patients. Long-term follow-up of these patients will be necessary to determine the persistence of these functional improvements and to evaluate the effects of treatment on retinal degeneration.

MATERIALS AND METHODS

Clinical Trial

This trial, registered under clinical trial number NCT01496040, is a phase 1/2 trial, and it was approved by the West Tours 1 ethics committee on March 4, 2011, and by the French Agency for Medicines and Healthcare Products on September 1, 2011. Patients provided written consent after they or their legal guardians were fully informed about the trial. Patients were split into three cohorts according to age and the dose of viral vector injected. Cohort 1 consisted of adult

patients who received the lowest dose of viral vector (up to 400 μL), whereas cohorts 2 (adult patients) and 3 (adult and pediatric patients) received a higher vector dose (up to 800 μL). An independent ethics committee responsible for approving the trial met between the treatment of patients 1 and 2, 3 and 4, 4 and 5, 6 and 7, and 7 and 8, to examine safety and tolerance data.

Patients

Each of the patients included in this study harbored two mutations in the *RPE65* gene, the presence of which was verified upon inclusion.

Vector Production

The pAAV-hRPE65 vector plasmid carries the transgene expression cassette flanked by AAV serotype 2 inverted terminal repeats (ITRs). The expression cassette contains the human *RPE65* coding sequence (NCBI RefSeq NM_000329) under the control of a human *RPE65* promoter fragment (positions −1,359 to +23 relative to the transcription start site) and a bovine growth hormone polyadenylation signal.

For production of the rAAV-2/4.hRPE65 vector, pAAV-hRPE65 plasmid was transfected into HEK293 cells together with pDP4-Kana helper plasmid, which provides both AAV serotype 4 *rep* and *cap* genes and adenovirus helper genes (VA RNA, E2A and E4). The vector was purified by ion-exchange chromatography and formulated in a saline solution specific for ocular surgery.

The rAAV-2/4.hRPE65 vector was aliquoted (0.5 mL) into 1.2 mL cryovials. The concentration of the final drug product, titered by dot blot hybridization, was 6×10^{10} vg/mL.

Surgery and Perioperative Treatment

Vector was administered by subretinal injection under general anesthesia into the eye with the greatest visual impairment. After a three-way 20G vitrectomy, the vector administration was performed using a 41G cannula as previously described.[15] The patient was immobilized for 20 min following surgery to maximize contact between the viral vector and RPE cells.

For 1 week before injection, patients received 0.5 mg/kg prednisolone per day (PO). This dosage was increased to 1 mg/kg/day for 1 week after surgery, and subsequently reduced over the following month before being stopped. Post-operative local treatment included dexamethasone-tobramycin eye drops, administered three times per day for 1 month, together with daily administration of 1% atropine eye drops for 7 days in the operated eye.

Evaluation of Viral Vector Dissemination

After surgery, patients were placed in a confinement chamber from D0 to D+3. Biodissemination of the AAV2/4.RPE65 vector was analyzed before and 1, 2, and 3 days after vector injection in nasal secretions and serum and urine samples. Analysis was performed by qPCR PREMIX EX TAQ (Perfect Real Time) TAKARA (Sigma) using the following primers/probes: Rev *polyA BGH* = 5′-AGG CAC AGT CGA GGC TGAT C-3′ (20-mer) (Sigma); *RPE65c-h* = 5′-GGT GAG CCC AGG AGC AGG ACA AAA GCC-3′ (27-mer); Fluo, FAM/TAMRA (Eurogentec). RNA extraction was performed using the QIAamp Viral RNA mini kit (QIAGEN) as follows: 1 cycle at 95°C for 10 min; 45 cycles at 95°C for 15 s; 45 cycles at 62°C for 30 s. The limit of detection was defined at 25 copies and the LOQ at 100 copies for nasal secretions and urine samples, and at 75 copies for serum samples.

Evaluation of Treatment Tolerance

A routine biomicroscopic ophthalmological examination of the anterior chamber and vitreal cavity and a biomicroscopic analysis of the retina were performed, and intra-ocular inflammation was scored according to the Nussenblatt rating system by measuring Tyndall protein levels in the anterior chamber with a LFM (Kowa FM700). Chorioretinal tolerance was evaluated by retinal photography with the ETDRS method, using a non-mydriatic retinograph (TOPCON TRC-NW6S) performed after pupil dilation with tropicamide (Ciba Vision Faure; Novartis). SD-OCT (Spectralis HRA-OCT; Heidelberg Engineering) was performed to analyze macular thickness, retinal structure, and nerve fiber thickness. Total retinal layer thickness was manually measured by two different operators at the fovea and 150, 300, and 600 μm along a horizontal line from the fovea, both temporally (0.5T, 1T, and 2T) and nasally (0.5N, 1N, and 2N), and statistical analyses were performed using R software version 3.0 (R Foundation for Statistical Computing). An angiographic examination (Spectralis HRA-OCT; Heidelberg Engineering) using fluorescein (5 mL of fluorescein sodium) and indocyanine green (Infracyanine; SERB) was performed to analyze vascular and retinal alterations following vector administration. Physical examinations and biochemical and hematological analyses were performed before and after vector administration.

Patients completed a tolerance questionnaire, providing information on ocular pain, ocular discomfort, and visual haziness following surgery.

Immunological Study

Humoral Responses to AAV4 Vector

Analyses were performed at the INSERM 1089 laboratory under our quality management system, which is approved by Lloyd's Register Quality Assurance (LRQA) to meet the requirements of International Management System Standards ISO 9001:2008. Anti-AAV4 IgG antibodies in patient sera were detected by ELISA using a method validated in accordance with ICH (Q2 R1) quality assurance guidelines. Briefly, patient serum samples were serially diluted in 0.1% PBS-Tween buffer and incubated in 96-well plates pre-coated with recombinant AAV2/4 viral particles. The reaction was revealed after incubation with peroxidase-conjugated donkey anti-human IgG $F(ab')_2$ fragment (Jackson ImmunoResearch) and tetramethylbenzidine (TMB) substrate (BD Biosciences). Optical densities were measured (450–570 nm) using a microplate spectrophotometer reader (Multiskan GO; Thermo Scientific). For each dilution, the positivity threshold was determined as the mean optical density + 3 SDs,

obtained independently by analysis of 19 negative sera samples from healthy donors. For positive samples, the IgG titer was defined as the highest serum dilution with an optical density remaining above the threshold curve.

Neutralizing factors against AAV4 were detected by neutralization assay. This assay is based on the inhibition of transduction in the COS cell line in the presence of serial serum dilutions using an AAV4 vector expressing the GFP reporter gene. Percentages of GFP-positive cells were determined by flow cytometry 72 hr after cell infection. The neutralizing titer was defined as the highest serum dilution that inhibited AAV transduction by $\geq$50% with respect to the transduction control without serum.

Cellular Immune Responses to AAV4 Vector and RPE65 Transgene Product

Cellular immune responses against AAV4 capsid and RPE65 gene product were evaluated using IFN-γ ELISpot assays and were performed at the immunology platform of Nantes University Hospital and, when necessary for some second sample runs, at the INSERM 1089 laboratory. Briefly, frozen peripheral blood mononuclear cells (PBMCs) were plated in 96-well ELIspot plates (Human IFN-γ ELISpot Plus kit; Mabtech) precoated with anti-IFN-γ and were stimulated in the presence of an overlapping peptide library at the final concentration of 2 μg/mL (Pepscreen; Sigma) covering either the AAV4 VP1 capsid protein sequence (split into three pools) or the RPE65 protein sequence (20 split into two pools). The reaction was revealed 24 hr after cell stimulation in accordance with the manufacturer's instructions (Human IFN-γ ELISpot Plus kit; Mabtech). Results were expressed as spot-forming colonies (SFCs)/10^6 cells. A positive response to any peptide pool was arbitrarily defined as any response >50 SFCs/10^6 cells and at least three times higher than the number of spots recorded in non-activated cells (medium alone).

Evaluation of Treatment Efficacy

Distance and close-range visual acuity were scored using the ETDRS and Parinaud scales, respectively. For distance visual acuity, statistical analyses were performed using BiostaTGV (Wilcoxon signed-rank test). Color vision was tested using the saturated 15-hue test in monocular vision. Visual field modifications were evaluated when visual acuity was greater than 20/200, using a visual field in automated perimetry (Octopus 101 Perimeter; Haag-Streit, Koeninz, Switzerland), together with a semi-static Goldmann analysis in V4. The surface area of visual fields was calculated using Allplan 2015 software. Next, we calculated two inter-individual ratios: V4 surface area at 1 year/V4 surface area at baseline, and V4 surface area at 2–3.5 years/V4 surface area at baseline. Statistical analyses were performed using R software 3.0 (R Foundation for Statistical Computing, Vienna, Austria). A microperimetry examination using a 4-2 strategy was performed after 10 min adaptation to darkness using 200-ms stimuli with a maximum luminance of 127 cd/m^2 (Nidek MP-1 Microperimeter; Nidek Technologies, Padova, Italy; NAVIS software, Version 1.7.1). A large-field ERG was performed following the International Society for Clinical Electrophysiology of Vision (ISCEV) protocol using a Monpack3 vision monitor (Metrovision, Perenchies, France). When fixation was of sufficient quality, a multifocal ERG was performed with the RETIscan system (Roland Consult, Wiesbaden, Germany) and RETIscan software (Version 3.15), in accordance with ISCEV recommendations. Pupil size, speed of dilatation, and pupil contraction in response to a series of flashes were measured by dynamic pupillometry using the Vision Monitor pupillometry device (Metrovision, Perenchies, France). To evaluate modification in mobility after subretinal vector administration, patients underwent a mobility test. The patient's travel time, through a maze using either the operated eye occluded or non-operated eye occluded, was measured in milliseconds and the number of mobility errors calculated. Patients were required to travel through the maze under two lighting conditions (4 lux and 240 lux). Each eye occlusion configuration was randomly selected. The test was performed three times for each lighting condition and each eye. A questionnaire on the patient's visual experience was taken after surgery. No test-retest variability was observed for any of the psychophysical assessments performed.

SUPPLEMENTAL INFORMATION

Supplemental Information includes Supplemental Materials and Methods and four tables and can be found with this article online at https://doi.org/10.1016/j.ymthe.2017.09.014.

AUTHOR CONTRIBUTIONS

G.L.M., F.R., and M.W. designed the experiments. P.M., C.D., and F.R. managed the vector production. S.B. and S.S. did the genetic testing. P.L. and R.V. proceeded with the functional MRI. O.A. conducted the immunological study. Y.P. supervised ERG testing. G.L.M., P.L., F.B., C.I., and M.W. realized investigations. M.W. performed surgery. G.L.M., P.L., and M.W. wrote the paper.

CONFLICTS OF INTEREST

G.L.M., P.M., and M.W. are members of the Scientific Council of Horama and serve on the scientific advisory board. The other authors have no conflicts of interest to declare.

ACKNOWLEDGMENTS

This study was supported by the AFM-Téléthon (Association Française contre les Myopathies). We extend our warmest gratitude to the patients who participated in this clinical trial, as well as their families. We thank the members of the PHRC06-08F (I. Audo, S. Defoort-Dhelemmes, H. Dollfus, C. Hamel, J. Kaplan, J. Sahel, and S. Mohand-Said) and the members of the ethics committee. We are grateful to A. Blériot for statistical analysis; C. Lejeune, D. Coeuru, and J.B. Ducloyer for the OCT study; S. Marconi for excel data; L. Callier for the visual field surface area study; C. Couzinié, M. Devaux, and I. Calard for immunological studies; and N. Provost, L. Libeau, A. Mendes-Madeira, E. Lhériteau, and C. Chauveau for the preclinical studies. We acknowledge N. Brument, S. Douthe, C. Robin, M. Enga, and A. François of the CPV (translational vector core) and ABG (Atlantic Bio GMP) for the production of the rAAV vectors. Finally, the authors thank the CIC-UIC12-Center of Clinical Research for logistic support.

REFERENCES

1. Leber, T. (1869). Ueber Retinitis pigmentosa und angeborene Amaurose. Graefes Arch. Clin. Exp. Ophthalmol. *15*, 1–25.
2. Kaplan, J. (2008). Leber congenital amaurosis: from darkness to spotlight. Ophthalmic Genet. *29*, 92–98.
3. Chacon-Camacho, O.F., and Zenteno, J.C. (2015). Review and update on the molecular basis of Leber congenital amaurosis. World J. Clin. Cases *3*, 112–124.
4. Hanein, S., Perrault, I., Gerber, S., Tanguy, G., Rozet, J.-M., and Kaplan, J. (2006). Leber congenital amaurosis: survey of the genetic heterogeneity, refinement of the clinical definition and phenotype-genotype correlations as a strategy for molecular diagnosis. Clinical and molecular survey in LCA. Adv. Exp. Med. Biol. *572*, 15–20.
5. Mata, N.L., Moghrabi, W.N., Lee, J.S., Bui, T.V., Radu, R.A., Horwitz, J., and Travis, G.H. (2004). Rpe65 is a retinyl ester binding protein that presents insoluble substrate to the isomerase in retinal pigment epithelial cells. J. Biol. Chem. *279*, 635–643.
6. Porto, F.B.O., Perrault, I., Hicks, D., Rozet, J.-M., Hanoteau, N., Hanein, S., Kaplan, J., and Sahel, J.A. (2002). Prenatal human ocular degeneration occurs in Leber's congenital amaurosis (LCA2). J. Gene Med. *4*, 390–396.
7. Jacobson, S.G., Cideciyan, A.V., Ratnakaram, R., Heon, E., Schwartz, S.B., Roman, A.J., Peden, M.C., Aleman, T.S., Boye, S.L., Sumaroka, A., et al. (2012). Gene therapy for leber congenital amaurosis caused by RPE65 mutations: safety and efficacy in 15 children and adults followed up to 3 years. Arch. Ophthalmol. *130*, 9–24.
8. Testa, F., Maguire, A.M., Rossi, S., Pierce, E.A., Melillo, P., Marshall, K., Banfi, S., Surace, E.M., Sun, J., Acerra, C., et al. (2013). Three-year follow-up after unilateral subretinal delivery of adeno-associated virus in patients with Leber congenital Amaurosis type 2. Ophthalmology *120*, 1283–1291.
9. Bainbridge, J.W.B., Smith, A.J., Barker, S.S., Robbie, S., Henderson, R., Balaggan, K., Viswanathan, A., Holder, G.E., Stockman, A., Tyler, N., et al. (2008). Effect of gene therapy on visual function in Leber's congenital amaurosis. N. Engl. J. Med. *358*, 2231–2239.
10. Banin, E., Bandah-Rozenfeld, D., Obolensky, A., Cideciyan, A.V., Aleman, T.S., Marks-Ohana, D., Sela, M., Boye, S., Sumaroka, A., Roman, A.J., et al. (2010). Molecular anthropology meets genetic medicine to treat blindness in the North African Jewish population: human gene therapy initiated in Israel. Hum. Gene Ther. *21*, 1749–1757.
11. Weleber, R.G., Pennesi, M.E., Wilson, D.J., Kaushal, S., Erker, L.R., Jensen, L., McBride, M.T., Flotte, T.R., Humphries, M., Calcedo, R., et al. (2016). Results at 2 years after gene therapy for RPE65-deficient Leber congenital amaurosis and severe early-childhood-onset retinal dystrophy. Ophthalmology *123*, 1606–1620.
12. Bainbridge, J.W.B., Mehat, M.S., Sundaram, V., Robbie, S.J., Barker, S.E., Ripamonti, C., Georgiadis, A., Mowat, F.M., Beattie, S.G., Gardner, P.J., et al. (2015). Long-term effect of gene therapy on Leber's congenital amaurosis. N. Engl. J. Med. *372*, 1887–1897.
13. Jacobson, S.G., Cideciyan, A.V., Roman, A.J., Sumaroka, A., Schwartz, S.B., Heon, E., and Hauswirth, W.W. (2015). Improvement and decline in vision with gene therapy in childhood blindness. N. Engl. J. Med. *372*, 1920–1926.
14. Bennett, J., Ashtari, M., Wellman, J., Marshall, K.A., Cyckowski, L.L., Chung, D.C., McCague, S., Pierce, E.A., Chen, Y., Bennicelli, J.L., et al. (2012). AAV2 gene therapy readministration in three adults with congenital blindness. Sci. Transl. Med. *4*, 120ra15.
15. Weber, M., Rabinowitz, J., Provost, N., Conrath, H., Folliot, S., Briot, D., Chérel, Y., Chenuaud, P., Samulski, J., Moullier, P., and Rolling, F. (2003). Recombinant adeno-associated virus serotype 4 mediates unique and exclusive long-term transduction of retinal pigmented epithelium in rat, dog, and nonhuman primate after subretinal delivery. Mol. Ther. *7*, 774–781.
16. Maguire, A.M., High, K.A., Auricchio, A., Wright, J.F., Pierce, E.A., Testa, F., Mingozzi, F., Bennicelli, J.L., Ying, G.S., Rossi, S., et al. (2009). Age-dependent effects of RPE65 gene therapy for Leber's congenital amaurosis: a phase 1 dose-escalation trial. Lancet *374*, 1597–1605.
17. Hoshi, S., Okamoto, F., Hasegawa, Y., Sugiura, Y., Okamoto, Y., Hiraoka, T., and Oshika, T. (2012). Time course of changes in aqueous flare intensity after vitrectomy for rhegmatogenous retinal detachment. Retina *32*, 1862–1867.
18. Murakami, Y., Yoshida, N., Ikeda, Y., Nakatake, S., Fujiwara, K., Notomi, S., Nabeshima, T., Nakao, S., Hisatomi, T., Enaida, H., and Ishibashi, T. (2015). Relationship between aqueous flare and visual function in retinitis pigmentosa. Am. J. Ophthalmol. *159*, 958–963.e1.
19. Veron, P., Leborgne, C., Monteilhet, V., Boutin, S., Martin, S., Moullier, P., and Masurier, C. (2012). Humoral and cellular capsid-specific immune responses to adeno-associated virus type 1 in randomized healthy donors. J. Immunol. *188*, 6418–6424.
20. Mingozzi, F., Maus, M.V., Hui, D.J., Sabatino, D.E., Murphy, S.L., Rasko, J.E.J., Ragni, M.V., Manno, C.S., Sommer, J., Jiang, H., et al. (2007). CD8(+) T-cell responses to adeno-associated virus capsid in humans. Nat. Med. *13*, 419–422.
21. Simonelli, F., Maguire, A.M., Testa, F., Pierce, E.A., Mingozzi, F., Bennicelli, J.L., Rossi, S., Marshall, K., Banfi, S., Surace, E.M., et al. (2010). Gene therapy for Leber's congenital amaurosis is safe and effective through 1.5 years after vector administration. Mol. Ther. *18*, 643–650.
22. Maguire, A.M., Simonelli, F., Pierce, E.A., Pugh, E.N., Jr., Mingozzi, F., Bennicelli, J., Banfi, S., Marshall, K.A., Testa, F., Surace, E.M., et al. (2008). Safety and efficacy of gene transfer for Leber's congenital amaurosis. N. Engl. J. Med. *358*, 2240–2248.
23. Hauswirth, W.W., Aleman, T.S., Kaushal, S., Cideciyan, A.V., Schwartz, S.B., Wang, L., Conlon, T.J., Boye, S.L., Flotte, T.R., Byrne, B.J., and Jacobson, S.G. (2008). Treatment of leber congenital amaurosis due to RPE65 mutations by ocular subretinal injection of adeno-associated virus gene vector: short-term results of a phase I trial. Hum. Gene Ther. *19*, 979–990.
24. Khanna, S., and Dell'Osso, L.F. (2006). The diagnosis and treatment of infantile nystagmus syndrome (INS). Sci. World J. *6*, 1385–1397.
25. Chung, S.T.L., LaFrance, M.W., and Bedell, H.E. (2011). Influence of motion smear on visual acuity in simulated infantile nystagmus. Optom. Vis. Sci. *88*, 200–207.
26. Koch, S.F., Tsai, Y.-T., Duong, J.K., Wu, W.-H., Hsu, C.-W., Wu, W.-P., Bonet-Ponce, L., Lin, C.S., and Tsang, S.H. (2015). Halting progressive neurodegeneration in advanced retinitis pigmentosa. J. Clin. Invest. *125*, 3704–3713.
27. MacLaren, R.E., Groppe, M., Barnard, A.R., Cottriall, C.L., Tolmachova, T., Seymour, L., Clark, K.R., During, M.J., Cremers, F.P., Black, G.C., et al. (2014). Retinal gene therapy in patients with choroideremia: initial findings from a phase 1/2 clinical trial. Lancet *383*, 1129–1137.
28. Kawamura, H., Fujikawa, M., Sawada, O., Sawada, T., Saishin, Y., and Ohji, M. (2016). Contrast sensitivity after pars plana vitrectomy: comparison between macula-on and macula-off rhegmatogenous retinal detachment. Ophthalmic Res. *56*, 74–78.
29. Rezar, S., Sacu, S., Blum, R., Eibenberger, K., Schmidt-Erfurth, U., and Georgopoulos, M. (2016). Macula-on versus macula-off pseudophakic rhegmatogenous retinal detachment following primary 23-gauge vitrectomy plus endotamponade. Curr. Eye Res. *41*, 543–550.
30. Kang, H.M., Lee, S.C., and Lee, C.S. (2015). Association of spectral-domain optical coherence tomography findings with visual outcome of macula-off rhegmatogenous retinal detachment surgery. Ophthalmologica *234*, 83–90.
31. Le Meur, G., Stieger, K., Smith, A.J., Weber, M., Deschamps, J.Y., Nivard, D., Mendes-Madeira, A., Provost, N., Péréon, Y., Cherel, Y., et al. (2007). Restoration of vision in RPE65-deficient Briard dogs using an AAV serotype 4 vector that specifically targets the retinal pigmented epithelium. Gene Ther. *14*, 292–303.
32. Aguirre, G.K., Komáromy, A.M., Cideciyan, A.V., Brainard, D.H., Aleman, T.S., Roman, A.J., Avants, B.B., Gee, J.C., Korczykowski, M., Hauswirth, W.W., et al. (2007). Canine and human visual cortex intact and responsive despite early retinal blindness from RPE65 mutation. PLoS Med. *4*, e230.
33. Hubel, D.H., and Wiesel, T.N. (1969). Anatomical demonstration of columns in the monkey striate cortex. Nature *221*, 747–750.
34. Striem-Amit, E., Ovadia-Caro, S., Caramazza, A., Margulies, D.S., Villringer, A., and Amedi, A. (2015). Functional connectivity of visual cortex in the blind follows retinotopic organization principles. Brain *138*, 1679–1695.
35. Tomaiuolo, F., Campana, S., Collins, D.L., Fonov, V.S., Ricciardi, E., Sartori, G., Pietrini, P., Kupers, R., and Ptito, M. (2014). Morphometric changes of the corpus callosum in congenital blindness. PLoS ONE *9*, e107871.

36. Ogawa, S., Takemura, H., Horiguchi, H., Terao, M., Haji, T., Pestilli, F., Yeatman, J.D., Tsuneoka, H., Wandell, B.A., and Masuda, Y. (2014). White matter consequences of retinal receptor and ganglion cell damage. Invest. Ophthalmol. Vis. Sci. *55*, 6976–6986.

37. Paul, D.A., Gaffin-Cahn, E., Hintz, E.B., Adeclat, G.J., Zhu, T., Williams, Z.R., Vates, G.E., and Mahon, B.Z. (2014). White matter changes linked to visual recovery after nerve decompression. Sci. Transl. Med. *6*, 266ra173.

38. Gawryluk, J.R., Mazerolle, E.L., and D'Arcy, R.C.N. (2014). Does functional MRI detect activation in white matter? A review of emerging evidence, issues, and future directions. Front. Neurosci. *8*, 239.

39. Ashtari, M., Zhang, H., Cook, P.A., Cyckowski, L.L., Shindler, K.S., Marshall, K.A., Aravand, P., Vossough, A., Gee, J.C., Maguire, A.M., et al. (2015). Plasticity of the human visual system after retinal gene therapy in patients with Leber's congenital amaurosis. Sci. Transl. Med. *7*, 296ra110.

YMTHE, Volume *26*

Supplemental Information

Safety and Long-Term Efficacy of AAV4 Gene Therapy in Patients with *RPE65* Leber Congenital Amaurosis

Guylène Le Meur, Pierre Lebranchu, Fanny Billaud, Oumeya Adjali, Sébastien Schmitt, Stéphane Bézieau, Yann Péréon, Romain Valabregue, Catherine Ivan, Christophe Darmon, Philippe Moullier, Fabienne Rolling, and Michel Weber

Supplementary Table 1.

	DNA allele 1	Protein 1	DNA allele 2	Protein 2
CG01	c.700C>T	p.Arg234X	c.1067delA	Asn356Methfs*17
BJ03	c.544C>G	p.His182Asp	c.726-2A>G	fs*
MM04	c.444G>C	p.Glu148Asp	c.1451G>A	p.Gly484Asp
MR05	c.74C>T	p.Pro25Leu	c.1301C>A	p.Ala434Glu
HM06	c.843_858+7del23	p.Asn282fs*	c.843_858+7del23	p.Asn282fs*
HT07	440_441delCA	p.Thr147Argfs*9	c.1448_1450delATG	p.Asp483del
AM08	246-11A>G	fs*	c.615_616delCA	p.Ile206Cysfs*27
HM09	c.989G>A	p.Cys330Tyr	c.843_858+7del23	p.Cys330Tyr
LC10	c.11+5G>A	fs*	c.1039C>T	p.Arg347Cys

Supplementary Table 2.

		D+1	D+2	D+3
BJ03	**lachrymal fluid**	4 (<LOD)	62 (<LOQ)	12 (<LOD)
HM06	**lachrymal fluid**	18 (<LOD)	7 (<LOD)	4 (<LOD)
HT07	**lachrymal fluid**	0	6 (<LOD)	0
HM09	**lachrymal fluid**	0	7 (<LOD)	16 (<LOD)
	blood	38 (<LOQ)	40 (<LOQ)	32 (<LOQ)
LC10	**lachrymal fluid**	6 (<LOD)	201	184

Supplementary Table 3.

		Anti-AAV 4 response			Anti-RPE65 response	
Patient	Day	Humoral (ELISA IgG)	Humoral (NF)	Cellular	Humoral	Cellular
CG01	BI	negative	negative	negative	non relevant results	negative
	D14					
	D30					
	D60					
	D120					
	D180					
BJ03	BI	negative	negative	negative		negative
	D14					
	D30					
	D60					
	D120					
	D180					
MM04	BI	negative	negative	positive (pools 1&2)		negative
	D14	1/10240	1/500			positive
	D30	1/10240	1/1000			positive
	D60	1/10240	1/1000			positive
	D120	1/10240	1/1000			negative
	D180	1/10240	1/1000			negative
MR05	BI	1/10240	1/50	negative		negative
	D14	1/10240	1/50			
	D30	1/2560	1/50			
	D60	1/10240	1/50			
	D120	1/10240	1/50			
	D180	1/10240	1/50			
HM06	BI	negative	negative	negative		negative
	D14					
	D30					
	D60					
	D120					
	D180					
HT07	BI	negative	negative	negative		negative
	D14					
	D30					
	D60					
	D120					
	D180					
AM08	BI	negative	negative	negative		negative
	D14					
	D30					
	D60					
	D120					
	D180					
HM09	BI	negative	negative	negative		negative
	D14	1/10240	1/1000			
	D30	1/10240	1/2500			
	D60	1/10240	1/2500			
	D120	1/10240	1/2500			
	D180	1/10240	1/2500			
LC10	BI	negative	negative	negative		negative
	D14					
	D30					
	D60					
	D120					
	D180					

Supplementary Table 4.

	treated eye	untreated eye
C1	0	0
C2	0	0
C3	- cerebellum	- thalamus (ipsilateral) - occipital lobe (contralateral)
C4	- precuneus (contralateral) - thalamus (ipsilateral) - corpus callosum - cerebellum	0
C5	- thalamus (ipsilateral)	0
C6	- thalamus (ipsilateral) - cerebellum	- frontal sup (contralateral)

Supplementary Table 1. Demographic and genetic characteristics of patients.

Supplementary Table 2. Vector genome values, as detected by qPCR in 5 patients during the biodistribution study (lachrymal fluid and blood samples).

Supplementary Table 3. Summary of the immunogical data collected during follow-up from the 9 patients. BI, baseline.

Supplementary Table 4. Clusters with a significantly higher activation after treatment according to light intensity and the side stimulated.

Supplementary Materials:

Functional MRI:

Each patient underwent an MRI before and 6 months after treatment. Visual stimulations were generated with the help of a specific software to monitor the lighting of images (Cogent, Matlab, The Mathworks, Inc., Natick, MA, USA). The images were projected (Epson EMP-8300 1024 x 768 pixels) onto a transparent stimulation screen (20.5° x 15°) placed 85 cm from the patient's eyes. We used a paradigm with a block design, alternating between different light stimulations (L) and rest in darkness (N). For each condition, monocular stimulation was performed by projecting onto the screen a homogeneous background

alternating between a grey and black value at a frequency of 5 Hz for 15 seconds. The luminance of the grey background was selected from 6 values (L1, L2, L3, L4, L5, L6), and remained unchanged for the 15-s presentation period, but varied from one value to another between presentations. L1 and L6 corresponded to minimum and maximum lighting values, respectively. Intermediate values (L2, L3, L4, L5) and were distributed homogeneously to cover the entire stimulation spectrum. The rest in darkness condition was set up by projecting a black background without visual or auditory stimulations for 15 seconds. During a run, the six conditions L and condition N were presented twice in a pseudorandom order (duration of a run = 3 minutes 30 seconds). Each patient performed 6 successive runs (3 right and 3 left monocular stimulations) during the acquisition session, with several minutes of rest between each run. The first eye stimulated was selected randomly, and the contralateral eye occluded with an ortopad. The same order of stimulation was always used (2 × eye 1, 2 × eye 2, 1 × eye 1, 1 × eye 2). The cache was changed between 2 runs. Functional acquisitions were performed with a 3-Tesla magnetic resonance system (32-channel Siemens Magnetom TrioTim syngo MR. VB13) and a standard 12-channel antenna placed around the head. During the MRI session, brain acquisition sections were oriented according to the AC-PC line. Functional data were acquired with T2-weighted gradient-EPI sequences (gradient-echo planar image; time repetition, 2800 ms; time echo, 30 ms; flip angle, 90°; matrix size, 80 x 80; field of view, 200 x 200 mm^2; voxel size, 2.5 x 2.5 x 2.5 mm^3; 50 transverse slices; 0.25 gap). Each run lasted 3.5 mins, enabling the acquisition of approximately 75 volumes. Two additional imaging sequences were acquired during the acquisition session. A T1-weighted anatomic acquisition (MP-RAGE) was performed, enabling superimposition of functional data on anatomic data. The acquisition session lasted approximately 1 hour. Functional data were analyzed using the SPM8 software (Wellcome Department of Cognitive Neurology, London, UK). The same pretreatment method was applied to all functional images acquired

(temporary resetting, correction of head movements, joint recording of anatomical and functional data, spatial normalization using the Montreal Neurological Institute (MNI) brain type, and spatial smoothing with the assistance of isotropic Gaussian kernels of 5-mm full-width at half-maximum (FWHM)) (1). In a first-level analysis, individual data were fitted to a general linear model (2). The model was designed to define for each of the 7 conditions (6L and 1N) a regressor describing the theoretic variation of the BOLD (blood oxygen level-dependent) signal during a run. This model was estimated and contrasts were then individually determined. The following contrasts were calculated using SPM8: C1=(L1-N), C2=(L2-N), C3=(L3-N), C4=(L4- N), C5=(L5-N), and C6=(L6-N). Positive effects of each contrast represent voxels significantly activated by luminosity stimulation (increasing intensity from L1 to L6) according to rest in the dark. Statistical parametric maps were thresholded at $P<0.05$ corrected for multiple comparisons using the familywise error (FWE) correction and for cluster extent at $P<0.05$. These analyses were performed separately for the treated eye (TE) and untreated eye (UTE) at each pre-and post-treatment session. For each stimulation condition, we determined for each patient the excess activation observed during the post-treatment session in regard to the pre-treatment session. Fixation in darkness remained the reference condition. Fixation in darkness remained the reference condition. The effect C1 of treatment during stimulation L1 was defined by contrast Cb1=(L1post-Npost) - (L1pre-Npré). Individual responses were variable both in terms of intensity (weak response of patients with the heaviest visual handicap) and topographic locations of activations within the visual cortex (3). We performed one analysis per region of interest. To characterize the functional properties of occipital region, we computed activity profiles plotting percentage signal change relative to “fixation in darkness”, averaged across subjects, under the different conditions. The primary visual cortex was defined as the region of interest (ROI) using a standardized map (WFU PickAtlas, Juelich Histological Atlas, BA17 R and L).

Simultaneously including the right and left parts of the primary visual cortex, the analysis included at the same time ipsilateral voxels for stimulation activated by direct ganglion fibers (temporary retina) and contralateral voxels for stimulations activated by crossed ganglion fibers (nasal retina). Therefore, the same ROI allowed comparison of results depending on whether the treated or contralateral eye was stimulated. The percentage voxel significantly activated for each contrast in ROI was extracted in addition to the average T score for the whole region. The analysis was performed with an initial threshold of $P<0.001$ for the detection of clusters of >10 voxels and confirmed with a second threshold of $P<0.1$ for the detection of clusters of >10 voxels so as not to disregard moderate effects. This has enabled setting out a parametric normogram representing the level of cortical activation (as intensity or as a percentage of voxels activated) according to luminance of light stimulation before and after treatment for the treated and control eye. One-way ANOVA was performed to observe a difference in activation according to stimulations conditions, subjects, treated or control eye (laterality) and timing of data acquisition (pre-or post-treatment). A three-way ANOVA with repeated measures with subject, laterality and timing condition as factors yielded significant main effects for the three factors, significant two-way interactions between each pair of factors, and a significant three-way interaction. To undertake group analyses, all data from patients treated on the left eye were inverted according to the axis xx'. This technique enables artificially defining the right eye as treated eye for all subjects, enabling coherent averaging of cortical activities for all patients. Voxels presenting more significant activation post-treatment in regard to pretreatment were sought in a group study using post-pre-individual results.

A second smoothing with a 5-mm FWHM isotropic Gaussian kernel was applied to the contrast images, and a random effect second-level group analysis was performed to assess the significance of activations at the population level (1). Statistical parametric maps were

thresholded at P <0.001 uncorrected with clusters of >15 voxels.

References:

1. Friston K, Frith C, Poline J-B, Heather J, Frackowiak R. Spatial registration and normalization of images. 1995;165–89.

2. Friston KJ, Holmes AP, Poline JB, Grasby PJ, Williams SC, Frackowiak RS, et al. Analysis of fMRI time-series revisited. NeuroImage. 1995 Mar;2(1):45–53.

3. Ogawa S, Takemura H, Horiguchi H, Terao M, Haji T, Pestilli F, et al. White matter consequences of retinal receptor and ganglion cell damage. Invest Ophthalmol Vis Sci. 2014 Oct;55(10):6976–86.